


Article

Interaction between a Sulfated Polysaccharide from Sea Cucumber and Gut Microbiota Influences the Fat Metabolism in Rats

Yujiao Zhang, Haoran Song, Zhengqi Liu, Chunqing Ai, Chunhong Yan, Xiuping Dong and Shuang Song * 

Liaoning Key Laboratory of Food Nutrition and Health, Collaborative Innovation Center of Seafood Deep Processing, National Engineering Research Center of Seafood, School of Food Science and Technology, Dalian Polytechnic University, Dalian 116034, China; zhangyujiao3@126.com (Y.Z.); 18104099219@163.com (H.S.); liuzhengqi@szu.edu.cn (Z.L.); acqdongying@163.com (C.A.); puniyan@foxmail.com (C.Y.); dxiuping@163.com (X.D.)

* Correspondence: songshuang@dlpu.edu.cn

Abstract: Due to its significant physiological effects, a sulfated polysaccharide has been considered an important nutrient of sea cucumber, but its metabolism in vivo is still unclear. The present study investigated the metabolism of a sea cucumber sulfated polysaccharide (SCSP) in rats and its influence on the metabolite profiles. The quantification by HPLC-MS/MS revealed that the blood level of SCSP achieved a maximum of $54.0 \pm 4.8 \mu\text{g/mL}$ at 2 h after gavage, almost no SCSP was excreted through urine, and $55.4 \pm 29.8\%$ of SCSP was eliminated through feces within 24 h. These results prove the utilization of SCSP by gut microbiota, and a further microbiota sequencing analysis indicated that the SCSP utilization in the gut was positively correlated with Muribaculaceae and Clostridia_UCG-014. In addition, the non-targeted metabolomic analysis demonstrated the significant effects of SCSP administration on the metabolite profiles of blood, urine, and feces. It is worth noting that the SCSP supplement decreased palmitic acid, stearic acid, and oleic acid in blood and urine while increasing stearic acid, linoleic acid, and γ -linolenic acid in feces, suggesting the inhibition of fat absorption and the enhancement of fat excretion by SCSP, respectively. The present study shed light on the metabolism in vivo and the influence on the fat metabolism of SCSP.

Keywords: marine polysaccharides; intestinal flora; nontargeted metabolomics



Citation: Zhang, Y.; Song, H.; Liu, Z.; Ai, C.; Yan, C.; Dong, X.; Song, S. Interaction between a Sulfated Polysaccharide from Sea Cucumber and Gut Microbiota Influences the Fat Metabolism in Rats. *Foods* **2023**, *12*, 4476. <https://doi.org/10.3390/foods12244476>

Academic Editor: Barry J. Parsons

Received: 15 November 2023

Revised: 7 December 2023

Accepted: 11 December 2023

Published: 14 December 2023



Copyright: © 2023 by the authors. Licensee MDPI, Basel, Switzerland. This article is an open access article distributed under the terms and conditions of the Creative Commons Attribution (CC BY) license (<https://creativecommons.org/licenses/by/4.0/>).

1. Introduction

Sea cucumber is valuable seafood, and it has been considered as a functional food and consumed traditionally in Asian countries, especially in China, Japan, and Korea [1]. A sea cucumber sulfated polysaccharide (SCSP) is the critical nutrient in sea cucumber, and it consists of two sulphated polysaccharides, namely fucosylated chondroitin sulphate and fucoidan sulphate [1,2]. The fucosylated chondroitin sulphate has a chondroitin core and a unique sulfated fucose side chain [3]. Fucoidan sulphate from sea cucumber is a linear polysaccharide consisting of $\alpha 1 \rightarrow 3$ linked fucose repeating units with various sulfation patterns [3]. SCSP has significant physiological effects such as anticancer [4], antibacterial activity [5], hypolipidemic [6], immune regulation [3,7] and anti-inflammation [8]. However, the underlying mechanism of its effects in vivo is still unclear. It has been proved that SCSP cannot be digested by gastrointestinal enzymes or acid liquid [9,10]. Moreover, as a macromolecule, it is difficult for SCSP to travel through intestinal epithelial cells, which could be inferred through the studies on other macromolecules [11]. Thus, more efforts are needed to reveal the action pathway of SCSP after oral supplementation.

Recently, more and more reports have verified that oral administration of indigestible polysaccharides could regulate gut microbiota so as to benefit the host health [12]. Our previous report has revealed that SCSP can effectively prevent diet-induced obesity through

modulating the composition of gut microbiota [13]. It has been proposed that indigestible polysaccharides can be metabolized by gut microbiota to produce bioactive metabolites, such as short-chain fatty acids, demonstrating beneficial effects on host health [14]. However, little evidence for the polysaccharide consumption by gut microbiota in vivo has been reported. Sulfated polysaccharides are more resistant to gut microbiota due to their sulfate groups [15,16]. Our previous study found that a part of SCSP could be fermented by fecal microbiota in vitro. But the utilization degree of SCSP by gut microbiota in vivo is still unknown.

Metabolomics have been widely used to analyze what occurs in diseases' process by identifying potential biomarkers and the related metabolic pathway [17]. However, increasing evidence has suggested that some metabolites produced by gut microbiota have potent functions for host energy metabolism [18,19]. Non-targeted metabolomics are a comprehensive approach for detecting metabolites as much as possible, and it is more robust in characterizing the metabolism profile and finding involved metabolites without targets [20]. Thus, in the present study, nontargeted metabolomics have been applied to monitor the regulation of SCSP on the metabolites in blood, urine, and feces to reveal the underlying action mechanism of SCSP.

The present study aimed to demonstrate the absorption, metabolism, and excretion of sea cucumber polysaccharides in vivo, and to analyze the effects of SCSP administration on the metabolite profiles of blood, urine, and feces, thus revealing the action pathway of sea cucumber polysaccharides in vivo.

2. Materials and Methods

2.1. Materials

The sea cucumber sulfated polysaccharide (SCSP) was extracted from *Stichopus japonicus* as previously reported [2]. This fraction (SCSP) was characterized in our previous study. It was composed of fucosylated chondroitin sulfate (179.4 kDa) and fucoidan (>670 kDa) with the mass ratio of 1.00:1.07, as evaluated by gel permeation chromatography (GPC). Furthermore, HPLC analyzed after acid hydrolysis and derivatization with PMP demonstrated that the molar ratio of sulfate/uronic acid/fucose (Fuc)/galactosamine (GalN) in SCSP was 7.6:0.8:9.1:1.0. 1-Phenyl-3-methyl-5-pyrazoline (PMP) was purchased from China National Pharmaceutical Group Co., Ltd. (Beijing, China). Trifluoroacetic acid, ammonium acetate, and formic acid were brought from Aladdin reagent Co., Ltd. (Shanghai, China). 1-Methylnicotinamide- d_3 iodide, acetyl-L-carnitine-(N-methyl- d_3), and DL-glutamic acid were purchased from Cambridge Isotope Laboratories Inc. (Cambridge, CA, USA). 12-[(Cyclohexylcarbonyl) amino] dodecanoic acid and chondroitin sulfate (shark) were both from Sigma-Aldrich Co. (St. Louis, MI, USA).

2.2. Animals

All animal experiments were performed in accordance with the guidelines for care and use of laboratory animals of Dalian Polytechnic University, and the experiment was approved by the Animal Ethics Committee of Dalian Polytechnic University (ID DLPU2018008).

Eighteen male Sprague Dawley (SD) rats (300 ± 20 g) were purchased from Liaoning Changsheng Biotechnology Company (Benxi, China). The rats were kept under standard conditions with a 12 h light–dark cycle, 23 ± 2 °C ambient temperature, and $55 \pm 10\%$ relative humidity. The feed was composed of corn, soybean meal, flour, bran, fish flour, salt, calcium hydrogen phosphate, rock flour, multivitamins, multiple trace elements, amino acids, etc., and more details are shown in Supplemental Table S5. The rats were acclimatized in clean cages for a fortnight prior to the experiment and weighed (310 ± 20 g), and then randomly divided into two groups: the Control group ($n = 9$) and the SCSP group ($n = 9$, named S1~S9).

To prevent the effects of food on SCSP absorption, the rats were fasted for 12 h before SCSP administration but drank water freely. The rats in the SCSP group were gavaged with 150 mg/kg of the SCSP solution (2 mL), and the Control group were gavaged with

the same volume of water. Then, the rats were put into metabolic cages and fed normally after 4 h. Fecal and urine samples were collected at 24 h and 48 h (frozen at $-80\text{ }^{\circ}\text{C}$) to ensure that SCSP was wholly excreted. After 1 day, 150 mg/kg of the SCSP solution was gavaged again. Then, the blood was extracted from the tail of the rats at 0 h, 0.5 h, 1 h, 2 h, 4 h, 6 h, 8 h, and 12 h after administration, and placed in centrifuge tubes containing an EDTA anticoagulant. At 24 h, the rats were anesthetized with ether, and blood samples were collected from the orbital vein and placed in centrifuge tubes containing the EDTA anticoagulant and ordinary centrifuge tubes. The coagulation time of the blood collected at 2 h after gavage from the broken tail of rats using a capillary was measured according to previously described reports [21,22].

2.3. Quantification of SCSP in Plasma, Feces, and Urine

Firstly, SCSP in plasma and feces was isolated. Plasma samples (0.1 mL) were suspended in a mixture of 0.5 mL of 2.6 M trifluoroacetic acid (TFA) and 0.4 mL of water. Dried fecal samples (0.20 g) were dissolved in 4 mL of water, and after centrifugation at 8000 rpm for 10 min, the supernatant (1 mL) was collected and mixed with ethanol (4 mL) and kept at $4\text{ }^{\circ}\text{C}$ overnight. Then, the precipitate was collected after centrifugation (4000 rpm, 10 min).

Quantification of SCSP was conducted as previously described [2]. Briefly, the collected precipitate containing SCSP was redissolved in water (5 mL). After that, 0.5 mL of the solution was mixed with 0.5 mL of 2.6 M TFA. Urine samples (10 mL) were concentrated to 1 mL using a rotary evaporator at $50\text{ }^{\circ}\text{C}$ under a vacuum. Then, a four-fold volume of ethanol was added, and the mixture stood at $4\text{ }^{\circ}\text{C}$ overnight. After that, the precipitate was collected by centrifugation (4000 rpm, 10 min), and dissolved in 1 mL of 1.3 M TFA.

Immediately after the above treatment, the samples were heated at $105\text{ }^{\circ}\text{C}$ for 3 h in sealed tubes for the acid hydrolysis. Then, the resulting solutions were dried with a vacuum concentrator (LaboGene Aps., Lyngø, Denmark). Then, 0.5 mL of methanol was added to the solution, which was dried again. This procedure was repeated thrice to remove TFA thoroughly. Then, 100 μL of 1 mg/mL lactose was added as an internal standard, and the mixtures were resolved in a solution composed of 400 μL of ammonia and 400 μL of a 0.3 M PMP methanolic solution. After heating at $70\text{ }^{\circ}\text{C}$ for 30 min in a water bath, the solution was dried with the vacuum concentrator. Thus, the PMP derivatives of hydrolysates of SCSP were prepared for an ESI-MS/MS analysis.

The chromatography separation was carried out on a Shimadzu HPLC system (LC-20ADXR pumps, SIL-20AXP Autosampler, Kyoto, Japan) with a Thermo Scientific (Waltham, MA, USA) Hypersil Gold column ($150 \times 2.1\text{ mm}$, $5\text{ }\mu\text{m}$). A 20 mM ammonium acetate solution and acetonitrile (85:15, *v/v*) were used as the mobile phase at a flow rate of 0.5 mL/min, and the column temperature was maintained at $30\text{ }^{\circ}\text{C}$. The ESI-MS/MS analysis was performed on a Q-trap 4000 triple-quadrupole mass spectrometer (AB Sciex, Framingham, MA, USA) in the positive-ion multiple reaction monitoring (MRM) mode. Mass spectrometry analysis parameters are provided in Supplemental Table S4.

2.4. Sequencing Analysis of the Gut Microbiota

Sequencing was carried out on an Illumina MiSeq PE250 platform (Novogene Genomics Technology Co., Ltd., Beijing, China, <https://magic.novogene.com> (accessed on 1 June 2021)). Briefly, Genomic DNA was isolated from fecal samples by the sodium dodecyl sulfate (SDS) method and assayed using agarose gel electrophoresis. After that, the genomic DNA was amplified with the 341F ($5'\text{-CCTACGGGNGGCWGCAG-3'}$) and 806R ($5'\text{-GGACTACHVGGGTWTCTAAT-3'}$) primers specific for the V3–V4 region of the 16S rRNA gene. Sequencing libraries were generated using the Ion Plus Fragment Library Kit 48 rxns and assessed on the Qubit@ 2.0 fluorometer (Thermo Scientific, Waltham, MA, USA). Alpha diversity and rarefaction curves were analyzed using QIIME V1.7.0. Venn diagrams were constructed using R software package V3.0.3 and were used to compare and analyze differences in the composition of OTUs in the intestinal flora between groups. A principal

coordinate analysis of PCoA and β -diversity was calculated using QIIME software V1.7.0 and presented using Stat, Ggplot2, and WGCNA packages in R software V2.15.3.

2.5. Analysis of Metabolites by UPLC-Q-TOF MS

According to the reported protocols [23], the serum sample (50 μ L), the urine sample (150 μ L), and the fecal sample (300 mg) were mixed with 200 μ L of methanol ($-20\text{ }^{\circ}\text{C}$), 300 μ L of water, and 500 μ L of a mixture (acetonitrile/methanol/water, 2:2:1, $v/v/v$), respectively. Then, 10 μ L of a mixed internal standard solution containing 20 ng/mL of 12-[(cyclohexylcarbonyl) amino] dodecanoic acid, 210 ng/mL of 1-methylnicotinamide- d_3 iodide, 51 ng/mL of acetyl-L-carnitine-(N-methyl- d_3), and 3500 ng/mL of DL-glutamic acid (2,4,4- d_3 , 98%) was added. The mixture was vortexed for 30 s, and then stored in a refrigerator at $-20\text{ }^{\circ}\text{C}$ for 30 min. After that, the mixture was centrifuged at 12,000 g/min for 5 min at $4\text{ }^{\circ}\text{C}$ and the supernatant was collected for a UPLC-Q-TOF MS analysis.

UPLC-Q-TOF MS analyses were performed on AB Sciex Triple TOF 5600 using both positive ion (PI) and negative ion (NI) modes. The chromatography separation was carried out using Waters Xselect @HSS T3 (2.5 μ m, 100 mm \times 2.1 mm) at a flow rate of 0.4 mL/min, and the column temperature was maintained at $30\text{ }^{\circ}\text{C}$. For the PI mode, the mobile phase was eluent A (0.1% formic acid in water, v/v) and eluent B (acetonitrile with 0.1% formic acid, v/v). For the NI mode, the mobile phase was eluent A (5 mM ammonium acetate in water) and eluent B (5 mM ammonium acetate in water/acetonitrile = 10:90, v/v). The solvent gradient was set as follows: 0–5 min, 0–20% B; 5–7 min, 20% B; 7–14 min, 20–100% B. The quality Control samples (QC) were prepared by mixing equal (10 μ L) amounts of each serum sample. The AB Sciex triple TOF 5600 mass spectrometer was operated with ion source gas 1 of 55 arb, ion source gas 2 of 55 arb, curtain gas of 35 arb, a temperature of $550\text{ }^{\circ}\text{C}$, and ion spray voltage floating of 5500 V for the PI mode and -4500 V for the NI mode.

The collected raw data were converted to “abf” format and the converted files were imported into MSDIAL. A principal component analysis (PCA) and orthogonal partial least squares discriminant analysis (OPLS-DA) were performed with SIMCA 14.1 software after exportation. And then the database in MSDIAL was used to identify the metabolites with a VIP value greater than 1.0.

2.6. Statistical Analysis

All data are expressed as means \pm standard deviations (SDs). Student’s *t*-test was used to evaluate the difference between two groups, and three groups were made by one-way ANOVA with Duncan’s test. $p < 0.05$ was considered to be significantly different. A multiple linear regression analysis was used to investigate the relationship between the utilization of SCSP and bacterial OTUs. Bacterial OTUs with $>1\%$ abundance were included in the regression model.

3. Results and Discussion

3.1. Absorption and Excretion of SCSP in Rats

In order to reveal the metabolism of SCSP in rats, SCSP in plasma, feces, and urine of rats after the gavage (46.5 mg) was quantified by HPLC-MS/MS. The method for the quantification of SCSP was validated for sensitivity, recovery, and repeatability (Supplemental Results). The results showed that the blood concentration of SCSP reached the maximum ($54.0 \pm 4.8\text{ }\mu\text{g/mL}$) at 2 h (Figure 1A). Since the circulating blood volume of rats is generally about 11 mL, it could be estimated that 1.2% SCSP was in blood circulation at that time. As shown in Table 1, SCSP in urine samples collected within 0~24 h and 24~48 h was nearly undetectable, and no more than 0.2% SCSP was excreted through urine as polymers. The same phenomenon has been previously reported [24]. Of note, $55.4 \pm 29.8\%$ of SCSP was detected in fecal samples within 24 h although there was great variability among individuals (Figure 1B). However, SCSP was barely detectable in feces after 24 h. From the above results, it could be concluded that the SCSP was mainly eliminated via feces within

24 h. Interestingly, a considerable proportion (~44%) of SCSP disappeared, indicating its degradation by intestinal flora. It has been reported that SCSP could be partially degraded by intestinal flora [25–27]. Moreover, the differences of SCSP contents in feces among rat individuals could be contributed to their diversity of intestinal microbiota communities [28]. As shown in Figure 1C, SCSP significantly prolonged coagulation time compared to the Control group ($p < 0.01$). Nadezhda E. Ustyuzhanina and R.J.C. Fonseca et al. had proved that fucosylated chondroitin sulfate in sea cucumber had an obvious anticoagulant effect by in vitro and in vivo experiments [29,30]. Our experiments also demonstrated the anticoagulant effect of gavaged SCSP, indicating that SCSP could be absorbed into the systemic circulation.

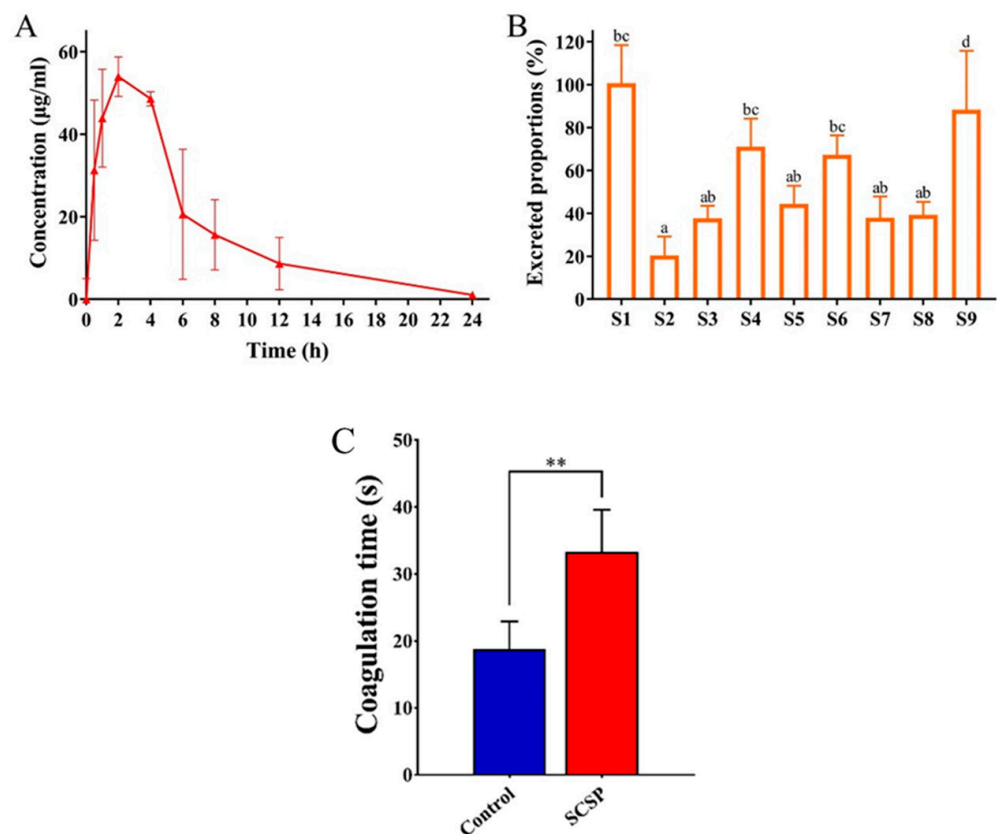


Figure 1. Mean plasma concentration–time profile of SCSP in rats after the gavage ($n = 3$, (A)), the excreted proportions of SCSP through feces within 24 h in different rat individuals (B), and the effect of SCSP on coagulation time in rats ($n = 3$, $** p < 0.01$, (C)). S1 to S9 stand for 9 rats making up different individuals. Graph bars marked with different letters on top represent statistically significant results ($p < 0.05$) based on one-way analysis of variance (ANOVA) followed by Duncan’s test, whereas bars labelled with the same letter correspond to results that show no statistically significant differences.

Table 1. Excreted amounts and ratios of SCSP in feces and urine.

Sample	Collecting Time (h)	0~24	24~48
Feces ($n = 9$)	SCSP amount (mg)	27.267 ± 14.662	0.0604 ± 0.083^a
	Excretion ratio (%)	55.42 ± 29.80	0.15 ± 0.17
Urine ($n = 3$)	SCSP amount (mg)	$<0.1^a$	$<0.1^a$
	Excretion ratio (%)	<0.2	<0.2

^a The data were not significantly different from those in Control group.

3.2. Relationship between Intestinal Flora and SCSP Utilization

The gut microbiota of the rats were analyzed through multiplex sequencing covering the V3–V4 regions of 16S rRNA, and the differences in the microbiota of the rat individuals were demonstrated. The relative abundances of microbiota at the phylum level (Figure 2A) showed that Bacteroidetes and Firmicutes were the dominant intestinal bacteria in these rats. The composition of Bacteroidetes was further demonstrated as shown in Figure 2B. Muribaculaceae was the most abundant family in Bacteroidetes, with an abundance of 85.2%, followed by Prevotellaceae (~10%) and Bacteroidae (~1%). Furthermore, the relative contributions of 35 dominant genera showed in the heatmap (Figure 2C) revealed that the composition of the intestinal flora varied greatly among individuals. The correlation between Operational Taxonomic Units (OTUs) and the utilization rate of SCSP was demonstrated by a multiple linear regression analysis (Supplemental Table S3) to obtain the regression model $y = 35.164x_1 + 38.257x_2 - 0.145$, where x_1 and x_2 are from Muribaculaceae and Clostridia_UCG-014, respectively. Thus, the result indicates the two OTUs were both positively correlated with the utilization rate of SCSP ($p < 0.05$).

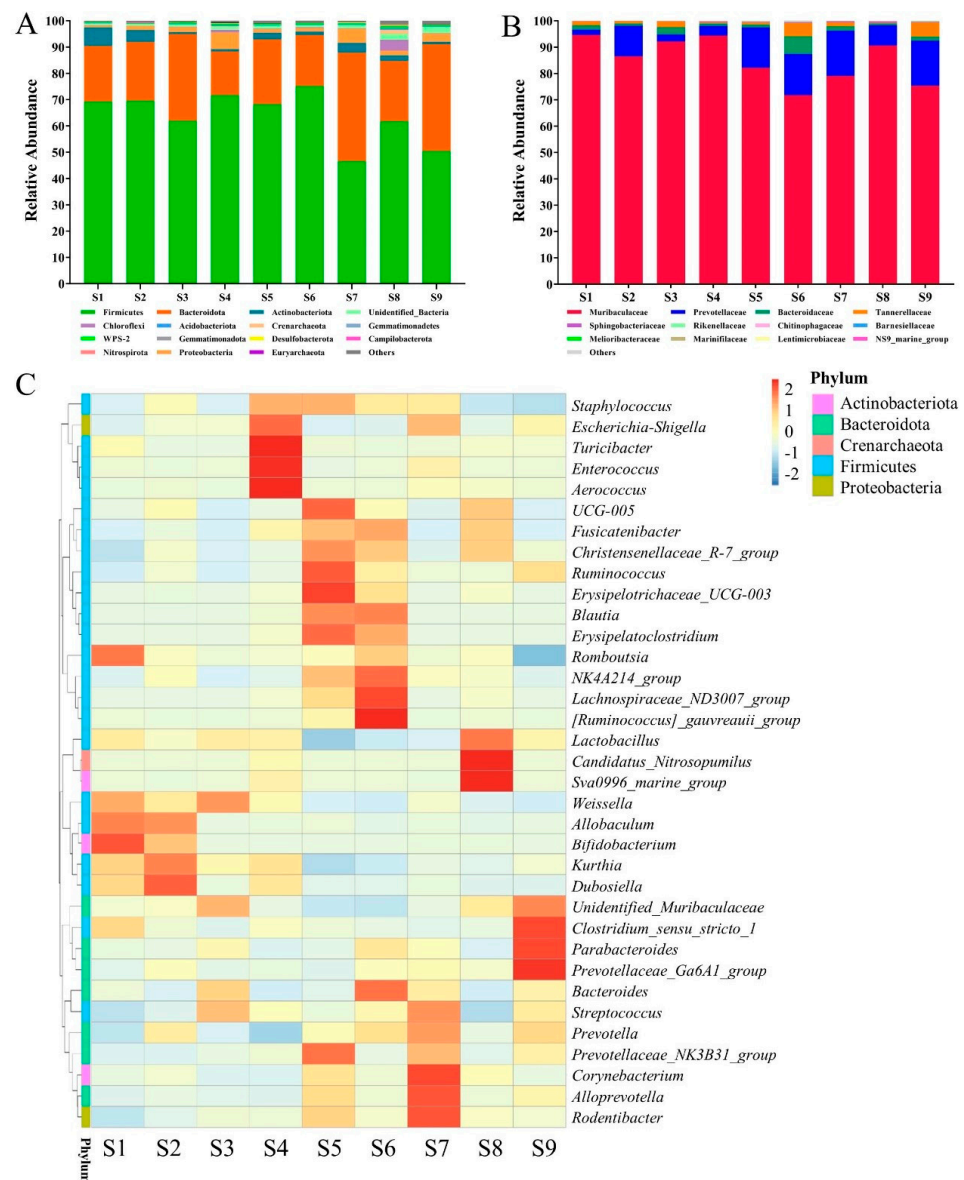


Figure 2. The relative abundances of intestinal microflora in different rats at the phylum level (A), the relative abundances of different families in Bacteroidota (B), and the heatmap of top 35 genera (C).

SCSP metabolism is a complex process that requires the participation of many gut microbes. It has been reported that some microorganisms such as *Bacteroides* and *Parabacteroides* are also involved in the metabolism of SCSP [27]. Different gut microbiota structures could respond to the intake food differently [27,31]. The discrepancy in the SCSP utilization in these rats could be attributed to the great diversity of their microbiota communities. Bacteroidetes, including Muribaculaceae, possess very large numbers of genes encoding carbohydrate-active enzymes, and are considered as the main contributors for polysaccharide utilization [32,33]. Muribaculaceae widely exist in the gut microbiota and a genome analysis indicated their potential capability to degrade complex carbohydrates [34]. Clostridia_UCG-014 has been identified as a member of Clostridiaceae, which possessed some well-studied cellulolytic organisms [35], and it has been considered as one of the major microbial contributors to digest polysaccharides due to its carbohydrate-degrading genes [36]. Then, the present study will suggest some bacteria from Muribaculaceae and Clostridiaceae that are keystone bacteria for SCSP utilization in the gut, affecting SCSP's outcome, such as anti-obesity and anti-type 2 diabetes [37].

3.3. Regulation of SCSP on Metabolite Profile of Feces

The effect of SCSP administration on the fecal metabolites was investigated through a non-targeted metabolomic analysis using Q-TOF-MS. As shown by PCA (Figure 3A) and OPLS-DA (Supplemental Figure S3), the fecal metabolite profiles of the SCSP group and the Control group separated with each other, indicating SCSP changed the metabolic profiles in the host gut. In total, 95 differential metabolites were identified in feces (Tables 2 and 3), and the related metabolic pathways with $-\log_{10}(p)$ and impact as the horizontal and vertical coordinates are shown in Figure 3B. The metabolic pathway obviously influenced by the SCSP supplement includes biosynthesis of unsaturated fatty acids, pantothenate and CoA biosynthesis, β -alanine metabolism, aminoacyl-tRNA biosynthesis, primary bile acid biosynthesis, riboflavin metabolism, linoleic acid metabolism, purine metabolism, histidine metabolism, retinol metabolism, arginine and proline metabolism, pyrimidine metabolism, tyrosine metabolism, and steroid hormone biosynthesis. Interestingly, the biosynthesis of unsaturated fatty acids and linoleic acid metabolism were both related to lipid metabolism. Of note, stearic acid, linoleic acid, and γ -linolenic acid in these two pathways were enriched by SCSP, indicating the enhancement of lipid metabolism in the guts of rats administrated SCSP.

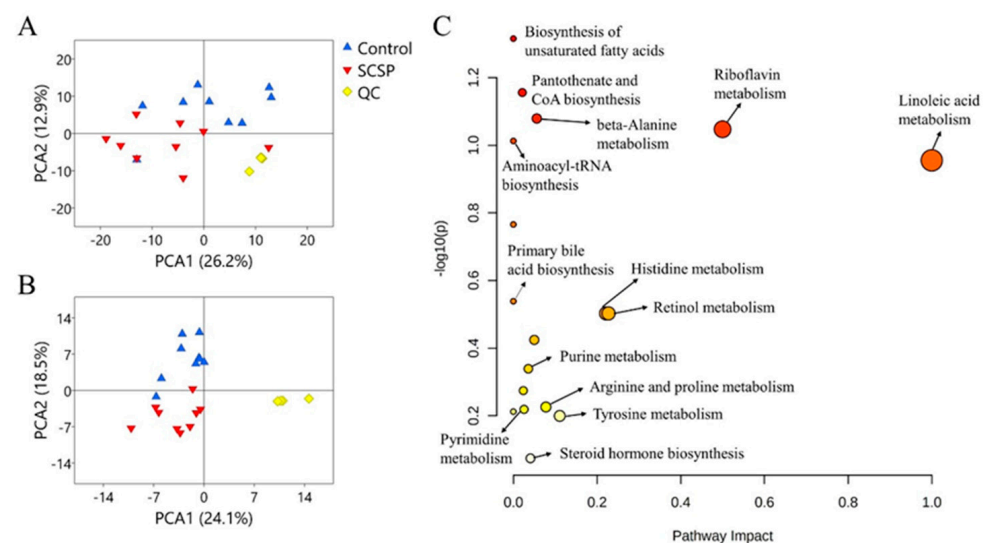


Figure 3. PCA analysis of the feces metabolites detected in the positive (A) and negative (B) modes and metabolism pathway analysis in rat feces (C).

Table 2. Identification results of differential metabolites in feces detected in the positive ion mode.

No.	Name	Formula	VIP	SCSP vs. Control
1	3-Amino-1,2,4-triazole	C ₂ H ₄ N ₄	1.37074	↑ (***)
2	Morpholine	C ₄ H ₉ NO	6.33961	↓
3	Diethanolamine	C ₄ H ₁₁ NO ₂	1.32672	↓ (**)
4	Dihydrouracil	C ₄ H ₆ N ₂ O ₂	1.14054	↑ (*)
5	L-proline	C ₅ H ₉ NO ₂	2.47750	↑ (***)
6	Valine	C ₅ H ₁₁ NO ₂	1.17142	↑ (*)
7	Cinnamaldehyde	C ₉ H ₈ O	1.89465	↓ (**)
8	2-Aminobenzimidazole	C ₇ H ₇ N ₃	1.41216	↑ (***)
9	Hypoxanthine	C ₅ H ₄ N ₄ O	1.58532	↓ (**)
10	Guanine	C ₅ H ₅ N ₅ O	1.22418	↓ (**)
11	His	C ₆ H ₉ N ₃ O ₂	1.14781	↑ (**)
12	2,8-Quinolinediol	C ₉ H ₇ NO ₂	2.45795	↑ (**)
13	Metronidazole	C ₆ H ₉ N ₃ O ₃	3.82603	↑ (*)
14	7,8-Dihydroxycoumarin	C ₉ H ₆ O ₄	1.67340	↑ (*)
15	5-Butylpyridine-2-carboxylic acid	C ₁₀ H ₁₃ NO ₂	1.14137	↓
16	Metamitron-desamino	C ₁₀ H ₉ N ₃ O	1.49271	↓
17	Levodopa	C ₉ H ₁₁ NO ₄	1.56546	↑
18	2-(4-Isobutylphenyl) propionic acid	C ₁₃ H ₁₈ O ₂	1.45771	↓ (*)
19	Pilocarpine	C ₁₁ H ₁₆ N ₂ O ₂	2.66077	↓ (***)
20	Terbumeton	C ₁₀ H ₁₉ N ₅ O	1.10183	↓ (*)
21	Flonicamid	C ₉ H ₆ F ₃ N ₃ O	3.03765	↓ (**)
22	Lumichrome	C ₁₂ H ₁₀ N ₄ O ₂	2.85914	↑ (**)
23	(2Z)-2-Benzylidene-6-methoxy-1-benzofuran-3(2H)-one	C ₁₆ H ₁₂ O ₃	1.40162	↓ (*)
24	Dehydroepiandrosterone	C ₁₉ H ₂₈ O ₂	2.13486	↓
25	Daidzein	C ₁₅ H ₁₀ O ₄	1.41342	↑ (**)
26	Epiandrosterone	C ₁₉ H ₃₀ O ₂	1.03079	↑
27	Jaeschkeanadiol	C ₁₅ H ₂₆ O ₂	1.06159	↓
28	Huperzine A	C ₁₅ H ₁₈ N ₂ O	2.14980	↑
29	Graveolide	C ₁₅ H ₂₀ O ₃	1.38494	↑ (**)
30	Baicalein	C ₁₅ H ₁₀ O ₅	1.68694	↓ (**)
31	Galaxolidone	C ₁₈ H ₂₄ O ₂	1.03394	↑ (*)
32	(-)-Eburnamonine	C ₁₉ H ₂₂ N ₂ O	1.93955	↑ (***)
33	All-trans-retinoic acid	C ₂₀ H ₂₈ O ₂	1.40410	↑ (*)
34	Methyl 3-(3,4-dihydroxy-5-phenyloxolan-2-yl)-3-hydroxypropanoate	C ₁₄ H ₁₈ O ₆	1.82178	↑
35	5-(4-Hydroxybenzyl)-4-(2-hydroxy-4-methoxyphenyl)-2(5H)-furanone	C ₁₈ H ₁₆ O ₅	1.05768	↓ (**)
36	5-(1,2,4a,5-Tetramethyl-7-oxo-3,4,8,8a-tetrahydro-2H-naphthalen-1-yl)-3-methylpentanoic acid	C ₂₀ H ₃₂ O ₃	1.23648	↓ (***)
37	Hydroquinidine	C ₂₀ H ₂₆ N ₂ O ₂	1.19523	↑ (***)
38	Raclopride	C ₁₅ H ₂₀ Cl ₂ N ₂ O ₃	1.19604	↓ (*)
39	Eicosanoids-bicycloPGE1	C ₂₀ H ₃₂ O ₄	2.81380	↓ (***)
40	Aphidicolin	C ₂₀ H ₃₄ O ₄	1.36684	↓ (*)
41	Melibiose	C ₁₂ H ₂₂ O ₁₁	2.25455	↓
42	(2E,4E)-12-Hydroxy-13-(hydroxymethyl)-3,5,7-trimethyltetradeca-2,4-dienedioic acid	C ₁₈ H ₃₀ O ₆	1.02162	↓
43	Hirsutine	C ₂₂ H ₂₈ N ₂ O ₃	1.12443	↓ (**)
44	4-(Hydroxymethyl)-1-isopropyl-3-cyclohexen-1-yl beta-D-glucopyranoside	C ₁₆ H ₂₈ O ₇	1.00738	↓
45	3-Methyl-5-(5,5,8a-trimethyl-2-methylene-7-oxodecahydro-1-naphthalenyl)pentyl acetate	C ₂₂ H ₃₆ O ₃	1.69849	↓
46	Deoxycholic acid	C ₂₄ H ₄₀ O ₄	1.00172	↑ (**)

Table 2. Cont.

No.	Name	Formula	VIP	SCSP vs. Control
47	(-)-Riboflavin	C ₁₇ H ₂₀ N ₄ O ₆	1.38226	↓ (*)
48	Methyl robustone	C ₂₂ H ₁₈ O ₆	3.32767	↑ (*)
49	Lagochilin	C ₂₀ H ₃₆ O ₅	1.12443	↓ (*)
50	Colladonine	C ₂₆ H ₃₂ O ₅	1.28344	↓ (**)
51	Voacristine	C ₂₂ H ₂₈ N ₂ O ₄	1.24153	↓ (**)
52	Cholic acid	C ₂₄ H ₄₀ O ₅	1.03719	↓
53	Monolinolein	C ₂₁ H ₃₈ O ₄	1.69026	↑ (**)
54	11,12-Methylenedioxykopsinaline	C ₂₂ H ₂₆ N ₂ O ₅	1.80736	↓
55	6-Hydroxy-2,4,4-trimethyl-3-(3-oxobutyl)-2-cyclohexen-1-yl beta-D-glucopyranoside	C ₁₉ H ₃₂ O ₈	1.74942	↓ (***)
56	2-Acetoxy-4-pentadecylbenzoic acid	C ₂₄ H ₃₈ O ₄	1.32797	↓
57	4,6',7'-Trihydroxy-6-(hydroxymethyl)-2',5',5',8a'-tetramethyl-3',4',4a',5',6',7',8',8a'-octahydro-2'H,3H-spiro[1-benzofuran-2,1'-naphthalene]-7-carbaldehyde	C ₂₃ H ₃₂ O ₆	4.20631	↑
58	Lovastatin M + Na	C ₂₄ H ₃₆ O ₅	1.20112	↓
59	Irbesartan	C ₂₅ H ₂₈ N ₆ O	1.00854	↓
60	Hyochoolic acid	C ₂₄ H ₄₀ O ₅	2.79818	↓
61	Beta-peltatin	C ₂₂ H ₂₂ O ₈	3.54980	↑
62	3-[5-Hydroxy-7-methoxy-2,3-dimethyl-6-(3-methylbut-2-enyl)-4-oxo-2,3-dihydrochromen-8-yl]hexanoic acid	C ₂₃ H ₃₂ O ₆	4.08549	↑ (**)
63	5-Hydroxy-5-(2-hydroxy-2-propanyl)-3,8-dimethyl-2-oxo-1,2,4,5,6,7,8,8a-octahydro-6-azulenyl β-D-glucopyranoside	C ₂₁ H ₃₄ O ₉	1.03474	↑
64	6-[3-[(3,4-Dimethoxyphenyl)methyl]-4-methoxy-2-(methoxymethyl)butyl]-4-methoxy-1,3-benzodioxole	C ₂₄ H ₃₂ O ₇	1.05174	↓
65	Prednisolone_tebutate	C ₂₇ H ₃₈ O ₆	1.53337	↓ (*)
66	Lunarine	C ₂₅ H ₃₁ N ₃ O ₄	1.10489	↓
67	Lycotoxine	C ₂₅ H ₄₁ NO ₇	1.02154	↓ (*)
68	NCGC00385237-01-C30H48O4	C ₃₀ H ₄₈ O ₄	1.03038	↓ (*)
69	Petunidin-3-O-beta-glucoside	C ₂₂ H ₂₃ O ₁₂	1.63603	↑ (*)
70	Emetine	C ₂₉ H ₄₀ N ₂ O ₄	1.08634	↓
71	(2R)-2-Hydroxy-3-(palmitoyloxy) propyl 2-(trimethylammonio)ethyl phosphate	C ₂₄ H ₅₀ NO ₇ P	1.13281	↓ (**)
72	1-Linoleoyl-2-hydroxy-sn-glycero-3-PC	C ₂₆ H ₅₀ NO ₇ P	1.45727	↓
73	Plasma ID-2759	C ₂₆ H ₅₂ NO ₇ P	1.05955	↓ (**)
74	Rhusflavone	C ₃₀ H ₂₂ O ₁₀	1.18525	↑
75	(1R,2R,3R,3aS,5aS,6R,7R,10R,10aR,10cR)-1,2,6,7-Tetrahydroxy-10a,10c-tetramethyl-4-oxo-6a,7,10,10a,10b,10c-dodecahydro-1H-phenanthro[10,1-bc] furan-10-yl beta-D-glucopyranoside	C ₂₅ H ₃₈ O ₁₂	2.23274	↓ (*)
76	Pantethine	C ₂₂ H ₄₂ N ₄ O ₈ S ₂	1.16095	↓
77	Cyanidin-3-O-sophoroside	C ₂₇ H ₃₁ O ₁₆	1.42677	↑ (*)
78	L-Glutathione	C ₂₀ H ₃₂ N ₆ O ₁₂ S ₂	1.06517	↑ (*)
79	Gitoxin	C ₄₁ H ₆₄ O ₁₄	3.23925	↑ (**)

Differential metabolites were analyzed using unpaired two-tailed Student's *t*-test with Bonferroni correction (* $p < 0.05$, ** $p < 0.01$, and *** $p < 0.001$ vs. the Control group; ↑, increase; ↓, decrease).

Table 3. Identification results of differential metabolites in feces detected in the negative ion mode.

No.	Name	Formula	VIP	SCSP vs. Control
1	Glyceraldehyde	C ₃ H ₆ O ₃	1.02494	↑ (**)
2	4-Hydroxybenzaldehyde	C ₇ H ₆ O ₂	1.48141	↓
3	Cis-Muconic acid	C ₆ H ₆ O ₄	1.90860	↓ (***)
4	Laurilsulfate	C ₁₂ H ₂₆ O ₄ S	1.70544	↓
5	γ-Linolenic acid	C ₁₈ H ₃₀ O ₂	1.68250	↑
6	Linoleic acid	C ₁₈ H ₃₂ O ₂	5.62134	↑ (***)
7	Stearic acid	C ₁₈ H ₃₆ O ₂	1.40114	↑ (*)
8	9,10-DiHOME	C ₁₈ H ₃₄ O ₄	1.48835	↓ (*)
9	7,15-Dihydroxyabieta-8,11,13-trien-18-oic acid	C ₂₀ H ₂₈ O ₄	1.11551	↓ (*)
10	5-[2-(Furan-3-yl) ethyl]-8-hydroxy-5,6,8a-trimethyl-3,4,4a,6,7,8-hexahydronaphthalene-1-carboxylic acid	C ₂₀ H ₂₈ O ₄	1.29029	↓
11	Lithochol-11-enic acid	C ₂₄ H ₃₈ O ₃	2.07634	↑ (**)
12	Lithocholic acid	C ₂₄ H ₄₀ O ₃	2.28879	↑ (**)
13	Deoxycholic acid	C ₂₄ H ₄₀ O ₄	4.56029	↓
14	Chenodiol	C ₂₄ H ₄₀ O ₄	5.97657	↓
15	Hyochoic acid	C ₂₄ H ₄₀ O ₅	6.87300	↓
16	Irbesartan	C ₂₅ H ₂₈ N ₆ O	1.39312	↑ (*)

Differential metabolites were analyzed using unpaired two-tailed Student's *t*-test with Bonferroni correction (* $p < 0.05$, ** $p < 0.01$, and *** $p < 0.001$ vs. the Control group; ↑, increase; ↓, decrease).

As we know, diet fat is digested and absorbed in the stomach and the small intestine [38]. More active lipid metabolism in the guts suggests more fat was transported to the gut without being absorbed by the upper digestive tract. Thus, the results in the present study indicate the supplementation of SCSP could inhibit the fat absorption. It has been reported that SCSP could prevent obesity induced by a high-fat diet [13], and the inhibition effect of SCSP against the fat absorption is one of the possible reasons for its anti-obesity activity. Liu et al. reported that the gut microbiota in HFD-fed mice were dominated by Muribaculaceae species, and the untargeted metabolomics analyses of fecal samples show that microbial changes altered the bacteria-derived metabolites, which related to linoleic acid metabolism [39]. Thus, it can be inferred that SCSP could interfere with linoleic acid metabolism by affecting Muribaculaceae to exert anti-obesity effects.

3.4. Regulation of SCSP on Metabolite Profiles of Serum and Urine

To evaluate the physiological effect of single gavage of SCSP, the metabolites in serum and urine of the rats were also determined by UPLC-Q-TOF MS in both positive and negative modes. As shown in Tables 4–7, 17 and 39 differential metabolites were identified in the serum and urine, respectively. The PCA analysis demonstrated a distinction between the serum metabolite profiles of the Control and SCSP groups in both of the positive (Figure 4A) and negative modes (Figure 4B). Moreover, although no significant separation was observed in urine profiles of the Control and SCSP groups detected in the positive mode (Figure 4C), the analysis result determined in the negative mode that an obvious separation was exhibited (Figure 4D). The separation between Control and SCSP groups demonstrated in the negative mode could be attributed to some acidic compounds, such as glycolic acid and arachidic acid. The metabolism pathway analysis in serum and urine metabolites is shown in Supplemental Figure S4. Thus, it can be concluded that single-dose SCSP administration can affect the in vivo metabolism of rats.

Table 4. Identification results of differential metabolites in serum detected in the positive ion mode.

No.	Name	Formula	VIP	SCSP vs. Control
1	Glycocyanine	C ₃ H ₇ N ₃ O ₂	1.84134	↓ (*)
2	3-Formylindole	C ₉ H ₇ NO	3.12390	↑
3	Phosphocholine	C ₅ H ₁₅ NO ₄ P	2.46685	↓ (***)
4	Phytosphingosine	C ₁₈ H ₃₉ NO ₃	1.55859	↑ (***)
5	Iprovalicarb	C ₁₈ H ₂₈ N ₂	3.53042	↓
6	LysoPC (18:3(9Z,12Z,15Z))	C ₂₆ H ₄₈ NOP	1.57622	↓ (***)
7	1-Linoleoyl-2-hydroxy-sn-glycero-3-PC	C ₂₆ H ₅₀ NOP	1.33664	↑
8	Isohernandezine	C ₃₉ H ₄₄ N ₂	1.41083	↓
9	(4R,9β,23E)-2-(β-D-Glucopyranosyloxy)-16,20-dihydroxy-9,10,14-trimethyl-1,11,22-trioxo-4,9-cyclo-9,10-secocholesta-2,5,23-trien-25-yl acetate	C ₃₈ H ₅₄ O ₁₃	1.02230	↑ (***)

Differential metabolites were analyzed using unpaired two-tailed Student's *t*-test with Bonferroni correction (* *p* < 0.05, and *** *p* < 0.001 vs. the Control group; ↑, increase; ↓, decrease).

Table 5. Identification results of differential metabolites in serum detected in the negative ion mode.

No.	Name	Formula	VIP	SCSP vs. Control
1	Lactic acid	C ₃ H ₆ O ₃	1.89469	↑ (*)
2	Palmitic Acid	C ₁₆ H ₃₂ O ₂	2.12223	↑ (**)
3	Oleic acid	C ₁₈ H ₃₄ O ₂	1.05400	↑
4	Stearic acid	C ₁₈ H ₃₆ O ₂	1.23960	↑
5	Thymol-β-D-glucoside	C ₁₆ H ₂₄ O ₆	1.62896	↑
6	9,10-DiHOME	C ₁₈ H ₃₄ O ₄	1.19020	↑ (**)
7	Hydroquinidine	C ₂₀ H ₂₆ N ₂ O ₂	1.72053	↑ (***)
8	19S-Methoxytubotaiwine	C ₂₁ H ₂₆ N ₂ O ₃	1.52218	↑

Differential metabolites were analyzed using unpaired two-tailed Student's *t*-test with Bonferroni correction (* *p* < 0.05, ** *p* < 0.01, and *** *p* < 0.001 vs. the Control group; ↑, increase).

Table 6. Identification results of differential metabolites in urine detected in the positive ion mode.

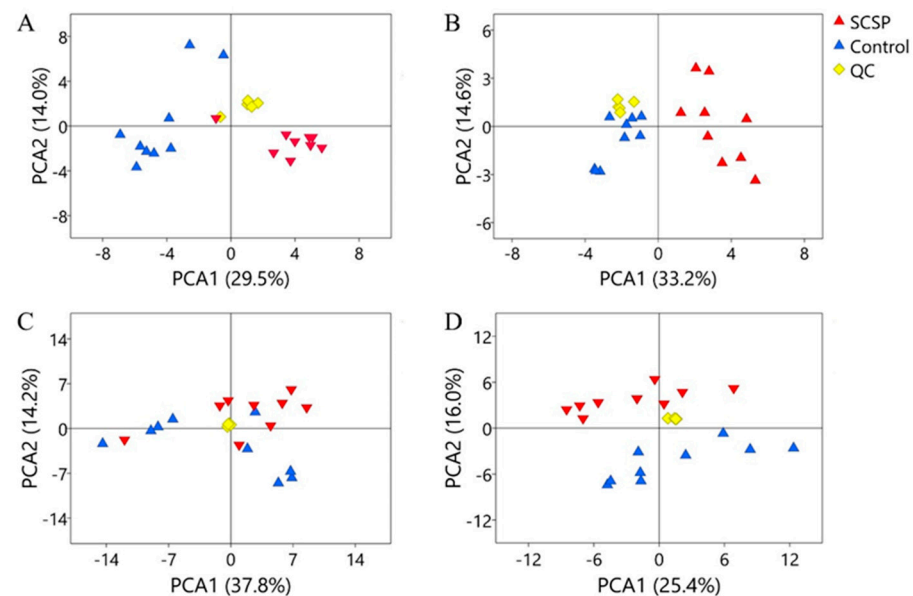
No.	Name	Formula	VIP	SCSP vs. Control
1	Pyrrrolidine	C ₄ H ₉ N	1.22976	↑ (***)
2	3-Amino-1,2,4-triazole	C ₂ H ₄ N ₄	3.94189	↑ (**)
3	D-Alanine	C ₃ H ₇ NO ₂	1.19995	↑ (*)
4	5-Methylcytosine	C ₅ H ₇ N ₃ O	2.25112	↑ (***)
5	2-Benzoxazolinone	C ₇ H ₅ NO ₂	1.82869	↑
6	3-Methyladenine	C ₆ H ₇ N ₅	1.69258	↑ (**)
7	7-Methanesulfinylheptanenitrile	C ₈ H ₁₅ NOS	1.57761	↑ (*)
8	Ethyl-4-dimethylaminobenzoate	C ₁₁ H ₁₅ NO ₂	2.53641	↑ (**)
9	Monuron	C ₉ H ₁₁ C ₁ N ₂ O	1.31887	↑ (*)
10	Thiabendazole	C ₁₀ H ₇ N ₃ S	1.43739	↓
11	Cyclo(proline-leucine)	C ₁₁ H ₁₈ N ₂ O ₂	1.25286	↑ (**)
12	Mefenamic acid	C ₁₅ H ₁₅ NO ₂	1.15207	↑
13	Estriol	C ₁₈ H ₂₄ O ₃	1.84057	↑ (**)
14	Daidzein	C ₁₅ H ₁₀ O ₄	1.88659	↓
15	Genistein	C ₁₅ H ₁₀ O ₅	1.82289	↑ (*)
16	Glycitein	C ₁₆ H ₁₂ O ₅	1.03938	↑
17	4'-Methylgenistein	C ₁₆ H ₁₂ O ₅	1.22976	↑ (*)
18	Adenosine 5'-monophosphate	C ₁₀ H ₁₄ N ₅ O ₇ P	2.49862	↑
19	Methyl (2E,4E,8E)-7,13-dihydroxy-4,8,12-trimethyltetradeca-2,4,8-trienoate	C ₁₈ H ₃₀ O ₄	1.03817	↑ (*)
20	2-(2,6-Dihydroxy-4-methoxycarbonylbenzoyl)-3-hydroxybenzoic acid	C ₁₆ H ₁₂ O ₈	1.27008	↑

Differential metabolites were analyzed using unpaired two-tailed Student's *t*-test with Bonferroni correction (* *p* < 0.05, ** *p* < 0.01, and *** *p* < 0.001 vs. the Control group; ↑, increase; ↓, decrease).

Table 7. Identification results of differential metabolites in urine detected in the negative ion mode.

No.	Name	Formula	VIP	SCSP vs. Control
1	Glycolic acid	C ₂ H ₄ O ₃	1.41701	↑ (***)
2	Catechol	C ₆ H ₆ O ₂	2.64152	↓
3	5-Methyl-1H-benzotriazole	C ₇ H ₇ N ₃	1.32223	↓
4	Ortho-aminobenzoic acid	C ₇ H ₇ NO ₂	1.17925	↓ (*)
5	4-Hydroxyquinoline	C ₉ H ₇ NO	1.07799	↓
6	2-Hydroxyacetanilide	C ₈ H ₉ NO ₂	1.25584	↑ (*)
7	Divarinol	C ₉ H ₁₂ O ₂	1.62192	↑ (***)
8	Allantoin	C ₄ H ₆ N ₄ O ₃	1.14447	↓
9	Saccharin	C ₇ H ₅ NO ₃ S	1.13550	↑
10	4-Pyridoxic acid	C ₈ H ₉ NO ₄	2.62819	↓
11	3-Indoxyl sulfate	C ₈ H ₇ NO ₄ S	1.82190	↓
12	Pantothenate	C ₉ H ₁₇ NO ₅	1.01748	↑ (*)
13	Daidzein	C ₁₅ H ₁₀ O ₄	2.82778	↑ (***)
14	9-Trans-palmitelaidic acid	C ₁₆ H ₃₀ O ₂	1.01288	↓ (***)
15	Trans-vaccenic acid	C ₁₈ H ₃₄ O ₂	4.77431	↓ (***)
16	Oleic acid	C ₁₈ H ₃₄ O ₂	3.37721	↓ (***)
17	Stearic acid	C ₁₈ H ₃₆ O ₂	2.22722	↓ (***)
18	8-(3-Octyl-2-oxiranyl) octanoic acid	C ₁₈ H ₃₄ O ₃	1.59172	↓ (***)
19	Arachidic acid	C ₂₀ H ₄₀ O ₂	1.36823	↓ (***)

Differential metabolites were analyzed using unpaired two-tailed Student's *t*-test with Bonferroni correction (* *p* < 0.05, and *** *p* < 0.001 vs. the Control group; ↑, increase; ↓, decrease).

**Figure 4.** PCA analysis of the serum and urine metabolites detected in the positive (A,C) and negative (B,D) modes.

Of note, palmitic acid, stearic acid, and oleic acid, which were all increased in the feces of the SCSP group, all decreased in serum and urine of the SCSP group. These long-chain fatty acids (LCFAs) are components of pork fat in the fodder, and they could be absorbed into serum [40]. Thus, the less serum LCFAs in the SCSP group indicated that SCSP could inhibit the LCFAs' absorption so as to increase fat excretion via feces. It has been reported that the dietary supplementation of SCSP could significantly reduce fat accumulation and lipid levels in high-fat-diet-fed mice [41]. Then, the findings in the present study suggest the inhibition of LCFAs' absorption plays a role in the anti-obesity and hypolipidemic effects of SCSP. It has been well documented that dietary fibers could prevent the absorption of fat by chelation with their micro-molecular chains [42]. Then, it could be inferred these SCSP

micromolecules may bind to fat in the intestine so as to interfere with the fat metabolism in the host.

Taking together all the above results, single gavage of SCSP in vivo could be proposed as follows: a proportion of SCSP could participate in various metabolic reactions of the rats to produce different metabolites, thus benefiting the host health. The other SCSP was not degraded, but they could reduce obesity and hyperlipidemia by inhibiting fat absorption and increasing fat excretion into the feces. This is consistent with the previous research result that SCSP can prevent diet-induced obesity and its associated diseases [13].

4. Conclusions

The present study demonstrated the absorption, the exertion, and the metabolism by gut microbiota of SCSP. As shown by the quantitative analysis of SCSP in blood, urine, and feces, only a small amount of SCSP could be absorbed into the blood while a proportion of SCSP was excreted in the feces, which suggests that a considerable proportion of SCSP was metabolized by gut microbiota and the metabolized amount of SCSP varied among individuals. The SCSP degradation in the intestine was positively correlated with Muribaculaceae and Clostridia_UCG-014, confirming the involvement of these gut bacteria in metabolism of SCSP in the gut. Furthermore, the changes of the metabolites in blood, urine, and feces caused by SCSP administration revealed that SCSP could inhibit the fat absorption by increasing fat excretion. Our findings provide a better understanding of the action mechanism of SCSP in vivo.

Supplementary Materials: The following supporting information can be downloaded at: <https://www.mdpi.com/article/10.3390/foods12244476/s1>. Supplemental Results 1 The validation of the method for quantification of SCSP. Supplemental Table S1 The LOD and LOQ of solid samples (dried sea cucumber) and liquid samples (sea cucumber wine). Supplemental Table S2 The recoveries of SCSP in solid samples (dried sea cucumber), liquid samples (sea cucumber wine), defatted feces, and undefatted feces. Supplemental Table S3 The coefficient of the regression model, which is about the correlation between OTUs with abundances $\geq 1\%$ and the utilization rate of SCSP. Supplemental Table S4 Mass spectrometry analysis parameters. Supplemental Table S5 Feed components (per kg of feed). Supplemental Figure S1 MRM chromatogram of PMP-fucose in plasma samples from the Control group (A) and the SCSP group (B), in urine samples from the Control group (C) and the SCSP group (D), and in fecal samples from the Control group (E) and the SCSP group (F). Supplemental Figure S2 The standard curve of PMP-fucose. Supplemental Figure S3 OPLS-DA of metabolites in feces detected in the positive (A) and negative (B) modes. Supplemental Figure S4 The metabolism pathway analysis in serum (A) and urine (B) metabolites.

Author Contributions: Y.Z.: Investigation, Data curation, Writing—original draft. H.S.: Formal analysis. Z.L.: Data curation. C.A.: Methodology. C.Y.: Writing—review and editing. X.D.: Project administration. S.S.: Conceptualization, Writing—original draft, Supervision, Project administration, Funding acquisition. All authors have read and agreed to the published version of the manuscript.

Funding: This work was funded by National Natural Science Foundation of China (No. 31972084).

Data Availability Statement: Data is contained within the article or supplementary material.

Conflicts of Interest: The authors declare no conflict of interest.

References

1. Xu, H.; Zhou, Q.; Liu, B.; Chen, F.; Wang, M. Holothurian fucosylated chondroitin sulfates and their potential benefits for human health: Structures and biological activities. *Carbohydr. Polym.* **2022**, *275*, 118691. [[CrossRef](#)] [[PubMed](#)]
2. Zhu, Z.; Zhu, B.; Ai, C.; Lu, J.; Wu, S.; Liu, Y.; Wang, L.; Yang, J.; Song, S.; Liu, X. Development and application of a HPLC-MS/MS method for quantitation of fucosylated chondroitin sulfate and fucoidan in sea cucumbers. *Carbohydr. Res.* **2018**, *466*, 11–17. [[CrossRef](#)] [[PubMed](#)]
3. Yang, D.; Lin, F.; Huang, Y.; Ye, J.; Xiao, M. Separation, purification, structural analysis and immune-enhancing activity of sulfated polysaccharide isolated from sea cucumber viscera. *Int. J. Biol. Macromol.* **2020**, *155*, 1003–1018. [[CrossRef](#)] [[PubMed](#)]

4. Liu, X.; Liu, Y.; Hao, J.; Zhao, X.; Lang, Y.; Fan, F.; Cai, C.; Li, G.; Zhang, L.; Yu, G. In vivo Anti-Cancer Mechanism of Low-Molecular-Weight Fucosylated Chondroitin Sulfate (LFCS) from Sea Cucumber *Cucumaria frondosa*. *Molecules* **2016**, *21*, 625. [CrossRef]
5. Shakouri, A.; Nematpour, F.; Adibpour, N.; Ameri, A. The Investigation of Anti-bacterial Activity of *Holothuria Leucospilota* Sea Cucumber Extracts (Body Wall, Guts and White Strings) at Chabahar Bay in Oman Sea. *Environ. Stud. Persian Gulf* **2014**, 135–140. Available online: <https://api.semanticscholar.org/CorpusID:53412840> (accessed on 14 November 2023).
6. Li, S.; Li, J.; Zhi, Z.; Wei, C.; Wang, W.; Ding, T.; Ye, X.; Hu, Y.; Linhardt, R.J.; Chen, S. Macromolecular properties and hypolipidemic effects of four sulfated polysaccharides from sea cucumbers. *Carbohydr. Polym.* **2017**, *173*, 330–337. [CrossRef]
7. Janakiram, N.B.; Mohammed, A.; Bryant, T.; Lightfoot, S.; Collin, P.D.; Steele, V.E.; Rao, C.V. Improved Innate Immune Responses by Frondanol A5, a Sea Cucumber Extract, Prevent Intestinal Tumorigenesis. *Cancer Prev. Res.* **2015**, *8*, 327. [CrossRef]
8. Wang, J.; Hu, S.; Jiang, W.; Song, W.; Cai, L.; Wang, J. Fucoidan from sea cucumber may improve hepatic inflammatory response and insulin resistance in mice. *Int. Immunopharmacol.* **2016**, *31*, 15–23. [CrossRef]
9. Imanari, T.; Washio, Y.; Huang, Y.; Toyoda, H.; Suzuki, A.; Toida, T. Oral absorption and clearance of partially depolymerized fucosyl chondroitin sulfate from sea cucumber. *Thromb. Res.* **1999**, *93*, 129–135. [CrossRef]
10. Zhao, L.; Qin, Y.; Guan, R.; Zheng, W.; Liu, J.; Zhao, J. Digestibility of fucosylated glycosaminoglycan from sea cucumber and its effects on digestive enzymes under simulated salivary and gastrointestinal conditions. *Carbohydr. Polym.* **2018**, *186*, 217–225. [CrossRef]
11. Ai, C.; Ma, N.; Sun, X.; Duan, M.; Wu, S.; Yang, J.; Wen, C.; Song, S. Absorption and degradation of sulfated polysaccharide from pacific abalone in in vitro and in vivo models. *J. Funct. Foods* **2017**, *35*, 127–133. [CrossRef]
12. Zhu, Z.; Zhu, B.; Sun, Y.; Ai, C.; Wu, S.; Wang, L.; Song, S.; Liu, X. Sulfated polysaccharide from sea cucumber modulates the gut microbiota and its metabolites in normal mice. *Int. J. Biol. Macromol.* **2018**, *120*, 502–512. [CrossRef]
13. Zhu, Z.; Zhu, B.; Sun, Y.; Ai, C.; Wang, L.; Wen, C.; Yang, J.; Song, S.; Liu, X. Sulfated Polysaccharide from Sea Cucumber and its Depolymerized Derivative Prevent Obesity in Association with Modification of Gut Microbiota in High-Fat Diet-Fed Mice. *Mol. Nutr. Food Res.* **2018**, *62*, e1800446. [CrossRef] [PubMed]
14. Li, L.; Yao, H.; Li, X.; Zhang, Q.; Wu, X.; Wong, T.; Zheng, H.; Fung, H.; Yang, B.; Ma, D.; et al. Destiny of Dendrobium officinale Polysaccharide after Oral Administration: Indigestible and Nonabsorbing, Ends in Modulating Gut Microbiota. *J. Agric. Food Chem.* **2019**, *67*, 5968–5977. [CrossRef] [PubMed]
15. Zhang, T.; Wu, S.; Ai, C.; Wen, C.; Liu, Z.; Wang, L.; Jiang, L.; Shen, P.; Zhang, G.; Song, S. Galactofucan from *Laminaria japonica* is not degraded by the human digestive system but inhibits pancreatic lipase and modifies the intestinal microbiota. *Int. J. Biol. Macromol.* **2021**, *166*, 611–620. [CrossRef] [PubMed]
16. Cartmell, A.; Lowe, E.C.; Baslé, A.; Firbank, S.J.; Ndeh, D.A.; Murray, H.; Terrapon, N.; Lombard, V.; Henrissat, B.; Turnbull, J.E.; et al. How members of the human gut microbiota overcome the sulfation problem posed by glycosaminoglycans. *Proc. Natl. Acad. Sci. USA* **2017**, *114*, 7037. [CrossRef] [PubMed]
17. McGarrah, R.W.; Crown, S.B.; Zhang, G.-F.; Shah, S.H.; Newgard, C.B. Cardiovascular Metabolomics. *Circ. Res.* **2018**, *122*, 1238–1258. [CrossRef]
18. Chávez-Talavera, O.; Tailleux, A.; Lefebvre, P.; Staels, B. Bile Acid Control of Metabolism and Inflammation in Obesity, Type 2 Diabetes, Dyslipidemia, and Nonalcoholic Fatty Liver Disease. *Gastroenterology* **2017**, *152*, 1679–1694.e3. [CrossRef]
19. McNabney, S.M.; Henagan, T.M. Short Chain Fatty Acids in the Colon and Peripheral Tissues: A Focus on Butyrate, Colon Cancer, Obesity and Insulin Resistance. *Nutrients* **2017**, *9*, 1348. [CrossRef]
20. Zeng, W.; Huang, K.-E.; Luo, Y.; Li, D.-X.; Chen, W.; Yu, X.-Q.; Ke, X.-H. Nontargeted urine metabolomics analysis of the protective and therapeutic effects of Citri Reticulatae Chachiensis Pericarpium on high-fat feed-induced hyperlipidemia in rats. *Biomed. Chromatogr.* **2020**, *34*, e4795. [CrossRef]
21. Ablat, N.; Ablimit, M.; Abudoukadier, A.; Kadeer, B.; Yang, L. Investigating the hemostatic effect of medicinal plant *Arnebia euchroma* (Royle) I.M. Johnston extract in a mouse model. *J. Ethnopharmacol.* **2021**, *5*, 114306. [CrossRef]
22. Carvalho, W.A.; Maruyama, S.R.; Franzin, A.M.; Abatepaulo, A.R.; Anderson, J.M.; Ferreira, B.R.; Ribeiro, J.M.; Moré, D.D.; Augusto Mendes Maia, A.; Valenzuela, J.G.; et al. *Rhipicephalus* (Boophilus) *microplus*: Clotting time in tick-infested skin varies according to local inflammation and gene expression patterns in tick salivary glands. *Exp Parasitol.* **2010**, *124*, 428–435. [CrossRef] [PubMed]
23. Pang, H.-H.; Jiang, M.-F.; Wang, Q.-H.; Wang, X.-Y.; Gao, W.; Tian, Z.-H.; Huang, J.-M. Metabolic profile of danshen in rats by HPLC-LTQ-Orbitrap mass spectrometry. *J. Zhejiang Univ.-Sci. B* **2018**, *19*, 227–244. [CrossRef] [PubMed]
24. Guimarães, M.A.M.; Mourão, P.A.S. Urinary excretion of sulfated polysaccharides administered to Wistar rats suggests a renal permselectivity to these polymers based on molecular size. *Biochim. Et Biophys. Acta (BBA)-Gen. Subj.* **1997**, *1335*, 161–172. [CrossRef]
25. Porter, N.T.; Martens, E.C. The Critical Roles of Polysaccharides in Gut Microbial Ecology and Physiology. *Annu. Rev. Microbiol.* **2017**, *71*, 349–369. [CrossRef] [PubMed]
26. Song, S.; Zhang, L.; Cao, J.; Xiang, G.; Cong, P.; Dong, P.; Li, Z.; Xue, C.; Xue, Y.; Wang, Y. Characterization of Metabolic Pathways and Absorption of Sea Cucumber Saponins, Holothurin A and Echinoid A, in vitro and in vivo. *J. Food Sci.* **2017**, *82*, 1961–1967. [CrossRef] [PubMed]

27. Liu, Z.; Zhang, Y.; Ai, C.; Wen, C.; Dong, X.; Sun, X.; Cao, C.; Zhang, X.; Zhu, B.; Song, S. Gut microbiota response to sulfated sea cucumber polysaccharides in a differential manner using an in vitro fermentation model. *Food Res. Int.* **2021**, *148*, 110562. [[CrossRef](#)] [[PubMed](#)]
28. Zhu, Z.; Han, Y.; Ding, Y.; Zhu, B.; Song, S.; Xiao, H. Health effects of dietary sulfated polysaccharides from seafoods and their interaction with gut microbiota. *Compr. Rev. Food Sci. Food Saf.* **2021**, *20*, 2882–2913. [[CrossRef](#)]
29. Ustyuzhanina, N.E.; Bilan, M.I.; Dmitrenok, A.S.; Silchenko, A.S.; Grebnev, B.B.; Stonik, V.A.; Nifantiev, N.E.; Usov, A.I. Fucosylated Chondroitin Sulfates from the Sea Cucumbers *Paracaudina chilensis* and *Holothuria hilla*: Structures and Anticoagulant Activity. *Mar. Drugs* **2020**, *18*, 540. [[CrossRef](#)]
30. Fonseca, R.; Mouro, P.A.S.J.T. Fucosylated chondroitin sulfate as a new oral antithrombotic agent. *Thromb. Haemost.* **2006**, *96*, 822–829. [[CrossRef](#)]
31. Fang, Q.; Hu, J.; Nie, Q.; Nie, S. Effects of polysaccharides on glycometabolism based on gut microbiota alteration. *Trends Food Sci. Technol.* **2019**, *92*, 65–70. [[CrossRef](#)]
32. Hao, Z.; Wang, X.; Yang, H.; Tu, T.; Zhang, J.; Luo, H.; Huang, H.; Su, X. PUL-Mediated Plant Cell Wall Polysaccharide Utilization in the Gut Bacteroidetes. *Int. J. Mol. Sci.* **2021**, *22*, 3077. [[CrossRef](#)] [[PubMed](#)]
33. McKee, L.S.; La Rosa, S.L.; Westereng, B.; Eijssink, V.G.; Pope, P.B.; Larsbrink, J. Polysaccharide degradation by the Bacteroidetes: Mechanisms and nomenclature. *Environ. Microbiol. Rep.* **2021**, *13*, 559–581. [[CrossRef](#)] [[PubMed](#)]
34. Lagkouvardos, I.; Lesker, T.R.; Hitch, T.C.A.; Gálvez, E.J.C.; Smit, N.; Neuhaus, K.; Wang, J.; Baines, J.F.; Abt, B.; Stecher, B.; et al. Sequence and cultivation study of Muribaculaceae reveals novel species, host preference, and functional potential of this yet undescribed family. *Microbiome* **2019**, *7*, 28. [[CrossRef](#)] [[PubMed](#)]
35. Jose, V.L.; Appoorthy, T.; More, R.P.; Arun, A.S. Metagenomic insights into the rumen microbial fibrolytic enzymes in Indian crossbred cattle fed finger millet straw. *AMB Express* **2017**, *7*, 13. [[CrossRef](#)]
36. Gong, G.; Zhou, S.; Luo, R.; Gesang, Z.; Suolang, S. Metagenomic insights into the diversity of carbohydrate-degrading enzymes in the yak fecal microbial community. *BMC Microbiol.* **2020**, *20*, 302. [[CrossRef](#)]
37. Zhao, F.; Liu, Q.; Cao, J.; Xu, Y.; Pei, Z.; Fan, H.; Yuan, Y.; Shen, X.; Li, C. A sea cucumber (*Holothuria leucospilota*) polysaccharide improves the gut microbiome to alleviate the symptoms of type 2 diabetes mellitus in Goto-Kakizaki rats. *Food Chem. Toxicol.* **2020**, *135*, 110886. [[CrossRef](#)]
38. Phan, C.T.; Tso, P. Intestinal lipid absorption and transport. *Front. Mol. Biosci.* **2001**, *6*, D299–D319. [[CrossRef](#)]
39. Liu, Y.; Yang, K.; Jia, Y.; Shi, J.; Tong, Z.; Fang, D.; Yang, B.; Su, C.; Li, R.; Xiao, X.; et al. Gut microbiome alterations in high-fat-diet-fed mice are associated with antibiotic tolerance. *Nat. Microbiol.* **2021**, *6*, 874–884. [[CrossRef](#)]
40. Nestel, P.; Clifton, P.; Noakes, M. Effects of increasing dietary palmitoleic acid compared with palmitic and oleic acids on plasma lipids of hypercholesterolemic men. *J. Lipid Res.* **1994**, *35*, 656–662. [[CrossRef](#)]
41. Hu, X.Q.; Xu, J.; Xue, Y.; Li, Z.J.; Wang, J.F.; Wang, J.H.; Xue, C.H.; Wang, Y.M. Effects of bioactive components of sea cucumber on the serum, liver lipid profile and lipid absorption. *Biosci. Biotechnol. Biochem.* **2012**, *76*, 2214–2218. [[CrossRef](#)] [[PubMed](#)]
42. Cummings, J.H. Nutritional implications of dietary fiber. *Am. J. Clin. Nutr.* **1978**, *31*, 521–529. [[CrossRef](#)] [[PubMed](#)]

Disclaimer/Publisher’s Note: The statements, opinions and data contained in all publications are solely those of the individual author(s) and contributor(s) and not of MDPI and/or the editor(s). MDPI and/or the editor(s) disclaim responsibility for any injury to people or property resulting from any ideas, methods, instructions or products referred to in the content.